

Achievement of Project 3: Evaluation of radiation budget on the basis of satellite data and ground observation network, and study of long-term changes in atmospheric parameters

Hiroaki Kuze¹, Tamio Takamura¹, and Naoko Saitoh¹

¹CEReS, Chiba University

1-33 Yayoi-cho, Inage-ku, Chiba 263-8522, Japan

hkuze@faculty.chiba-u.jp, takamura@faculty.chiba-u.jp

Abstract

The long-term changes in the radiation budget of the East Asia region and related atmospheric parameters have been investigated in a comprehensive manner, employing both the satellite data and ground-network data. Through the recent activities of this project, new algorithms have been developed and tested for extracting various atmospheric parameters from satellite data. Simultaneous observations with ground instruments, including a network observation called SKYNET, are used for validation as well as improvement of the algorithms. Regional and seasonal variations of aerosol, cloud, and radiation amounts have been studied.

Keywords : atmospheric remote sensing, radiation budget, aerosol, cloud, atmospheric correction, satellite observation, calibration, ground observation, GOSAT, greenhouse gases

1. Introduction

The satellite evaluation of radiation budget in the Earth's surface system provides basic quantities required for the study of the global climate change including model studies. The accurate understanding of radiation budget is indispensable for studying dynamic behavior of vegetation, hydrology, and ocean environment. The purpose of this project is to investigate the long-term changes in the radiation budget of the East Asia region and related atmospheric parameters in a comprehensive manner, employing both the satellite data and ground-network data. Details of recent achievements will be described in the following sections.

2. Variations of atmospheric parameters and long-term radiation budget using remote sensing data

2.1 Algorithm development for radiation budget studies

Land surface albedo is a key parameter in radiation budget and climate modeling studies. An empirical anisotropy correction model for estimating land surface albedo has been developed for snow free land surfaces under clear sky conditions.¹⁾ The proposed model can be used for direct

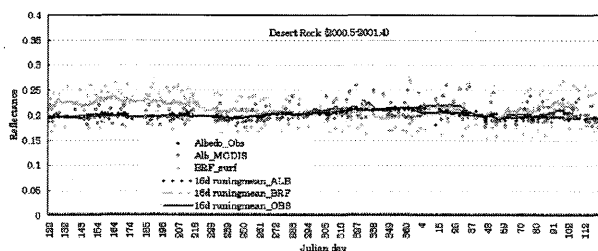


Fig. 1 Comparison of MODIS and surface albedo¹⁾

esti

mation of surface albedo from a single BRF observation (Fig. 1). The cloud optical thickness (COT) derived from the GMS-5/SVISSR is examined to estimate short-wave radiation budget. By comparing with MODIS COT, the GMS-5-retrieved COT has been corrected.²⁾

2.2 Measurement of time-integral of photosynthesis for NPP estimation in Mongolia

We applied the monthly mean PAR for vegetation photosynthesis to estimate the NPP from Landsat ETM+ data for a semi-arid area of Mongolia.³⁾ The estimated NPP results were compared with ground measurement data.

2.3 Long-term characterization of seasonal variation of tropospheric aerosols in Chiba

Seasonal variations of tropospheric aerosol properties in Chiba, Japan, are investigated by means of sunphotometer measurement (1999–2005) (Fig. 2), ground sampling (1998–2004), and wind data.⁴⁾ The influence of anthropogenic particles from local sources as well as that of Asian dust particles have been detected and discussed. The seasonal variation is remarkable also in the chemical analysis data.

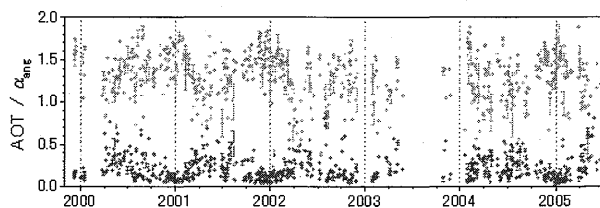


Fig. 2 Long-term variations of aerosol optical thickness (AOT) at 500nm (green) and Angstrom exponent (orange) Average values around noon are plotted.⁴⁾

2.4 Estimation of shortwave radiation budget using ADEOS II/GLI data

The downward and upward solar radiation at the surface and at the top of the atmosphere are estimated using GLI aerosol and cloud products.⁵⁾ The ground-observed data using i-sky radiometer are used for evaluating the satellite-derived aerosol and cloud products.

3. Collection of ground-validation data and improvement in satellite data analysis

3.1 Dual-site lidar observations and satellite data analysis for regional cloud characterization

Lidar data observed by two continuously operated portable automated lidar (PAL) systems and images from the visible and thermal infrared channels of AVHRR sensor onboard NOAA16 satellite are employed for the characterization of cloud heights and cloud types.⁶⁾

3.2 Influence of inhomogeneous cloud fields on satellite observations

GMS-5/SVISSR-retrieved cloud optical depth (COD) appeared mostly lower than that of Terra-MODIS.⁷⁾ The major factors causing such COD differences are the satellite viewing and solar conditions, the cloud thermodynamic phase differentiation and particle effective radius, and the cloud inhomogeneity. Here the emphasis is put on the examination of the cloud inhomogeneity effect.

3.3 A high-efficiency aerosol scatterometer for the calibration of multi-wavelength lidar data

A scatterometer (Fig. 3) was developed to measure the aerosol scattering coefficient at the ground level, on the basis of an integrating sphere, cw lasers, and a controlled flow of the ambient air, including aerosol particles.⁸⁾

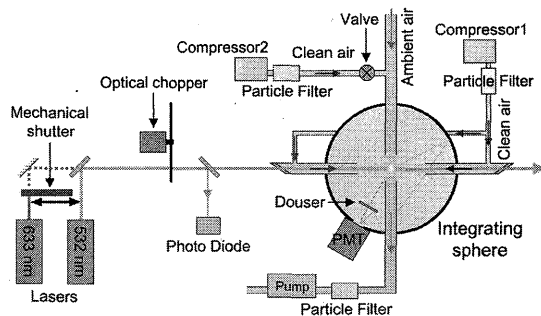


Fig. 3 Aerosol scatterometer based on an integrating sphere.

3.4 Aerosol mass extinction efficiency studied by continuous

lidar measurements

Continuous data of the atmosphere monitored using a portable automated lidar are correlated with the concentration of ground-measured suspended particulate matter (SPM).⁹⁾ When the boundary layer is well mixed, high correlation makes it possible to calculate the mass extinction efficiency of the aerosols in the atmosphere.

3.5 The influence of ambient humidity on the aerosol mass concentration measurements

The influence of humidity is considered on the concentration of the suspended particulate matter measured with a β -ray counter.¹⁰⁾ For the monthly data taken in September 2005, the difference in relative humidity between inside the instrument (48%) and outside the laboratory (78%) resulted in approximately 53% larger aerosol mass concentration after the correction, also affecting the mass extinction efficiency.

4. Analysis of atmospheric environment based on ground-network observations

4.1 Intercomparison between lidar and airborne measurements near Tokyo during ACE-Asia

In April 2001 during the ACE-Asia campaign, intercomparison studies were carried out near Tokyo using ground-based lidar networks as well as aircraft observations. Modest concentrations of Asian dust in the free troposphere was found to extend up to an altitude of 8 km.¹¹⁾

4.2 Study of atmospheric brown cloud and its radiative effect

Simultaneously measured sky-radiation and surface-solar-flux data are used to retrieve aerosol optical properties. Data sets from several SKYNET sites suggest that Asian dusts become blackened during the movement because of mixing with soot particles produced over the industrial/urban area of China.¹²⁾ In a campaign conducted on Cheju Island, Korea, the values of aerosol radiative forcing suggest that the aerosols might consist of more or less yellow sand in comparison with the results simulated using typical aerosol models (Fig. 4).¹³⁾

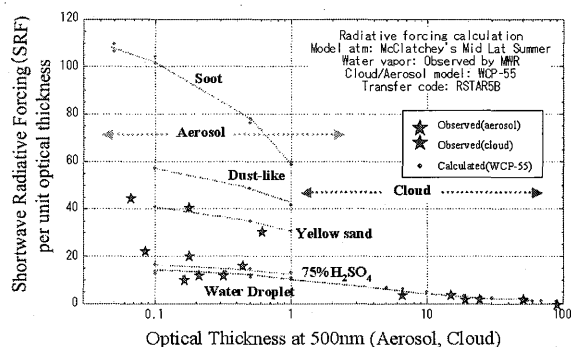


Fig. 4 Shortwave radiative forcing vs. optical thickness.

4.3 Aircraft and ground-based observations of boundary layer CO₂ concentration

Concentrations of atmospheric CO₂ and aerosol were measured in a field campaign conducted in winter 2006 around Mt. Tsukuba, Japan using ground-based CO₂ analyzers, a lidar, and sky radiometers as well as CO₂ analyzers onboard an aircraft.¹⁴⁾ A sudden increase of downward winds, due to the approach of an anticyclonic synoptic flow, resulted in a rapid decrease in both the CO₂ and aerosol concentrations in the boundary layer.

5. Development of algorithm for retrieving CO₂ vertical profiles from GOSAT satellite

5.1 Greenhouse gases observing satellite/thermal and near infrared sensor for carbon observation

The Greenhouse Gases Observing Satellite (GOSAT) is a sun-synchronous orbital satellite developed by NIES, Ministry of Environment, and JAXA for global observations of greenhouse gases.¹⁵⁾ The satellite was successfully launched from the Tanegashima Space Center in Japan on 23 January 2009. The GOSAT completed its system checkout, and started its regular operational observations, including both nadir and off-nadir measurements, of approximately 56,000 ground points every three days. It carries two sensors: the Thermal and Near Infrared Sensor for Carbon Observation (TANSO)-FTS and the TANSO-Cloud and Aerosol Imager (CAI). The former is a Fourier transform spectrometer that measures near infrared and thermal infrared radiances for detecting atmospheric gases. The latter is an imager to detect clouds and aerosols in the instantaneous field of view (IFOV) of the TANSO-FTS. The TANSO-FTS consists of four spectral bands: Band 1 (0.75-0.78 μm), Band 2 (1.56-1.72 μm), Band 3 (1.92-2.08 μm), and Band 4 (5.5-14.3 μm)¹⁶⁾. The maximum optical path difference of the TANSO-FTS is ± 2.5 cm; thus, the full width at half maximum of the instrumental line shape (spectral resolution) is approximately 0.2 cm^{-1} . We use the Band 4 spectra, which include CO₂ absorption band from 700 to 800 cm^{-1} (hereafter referred to as the “CO₂ 15- μm band”).

5.2 Retrieval methods

A non-linear maximum *a posteriori* (MAP) method¹⁷⁾ is adopted to retrieve CO₂ vertical profiles from the CO₂ 15- μm band. In the CO₂ retrieval, we introduce linear mapping between vertical layer grids for radiative transfer calculation (hereafter referred to as “full grids”) and grids for

CO₂ retrieval (“retrieval grids”). We divide the atmosphere from 1100 to 0.1 hPa into 110 layers, and define the layers as the full grids. We define the retrieval grids on the basis of the CO₂ averaging kernel functions. We select channels for the CO₂ retrieval using CO₂ information content in the CO₂ 15- μm band. Through CO₂ retrieval simulations, we confirmed that selecting 100 channels on the basis of CO₂ information content for all layers, 10 channels for the region above 55 hPa, and 50 channels for the region below 800 hPa was sufficient to achieve CO₂ retrieval with 1% accuracy from the troposphere through the stratosphere. In the CO₂ retrieval, uncertainties in the estimates of profiles of temperature, water vapor, and ozone are considered as a part of measurement spectral noise. For the GOSAT operational data processing, outputs from the NIES transport model¹⁸⁾ are used as *a priori* CO₂ profiles. The *a priori* error covariance matrix is determined from errors in the NIES transport model¹⁹⁾.

5.3 Preliminary CO₂ retrieval results

We now analyze the interferograms obtained by the TANSO-FTS to determine several correction parameters for a nonlinearity correction and a phase correction. Although several adjustments based on its in-orbit calibrations have to be applied to the interferograms, we retrieved CO₂ profiles from the not-well calibrated Band 4 spectra by using the

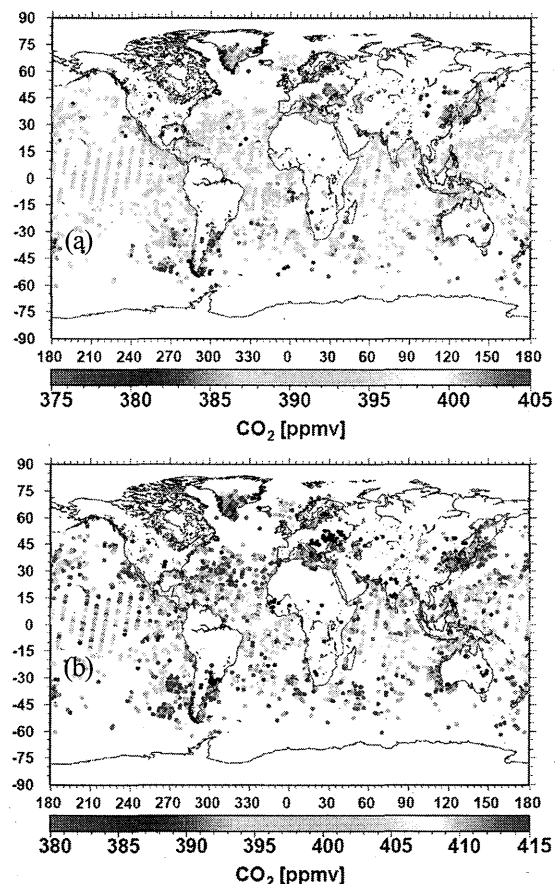


Fig. 5 CO₂ concentrations retrieved from the TANSO-FTS Band 4 spectra obtained from April 6 to 8, 2009 on (a) 770 hPa pressure level; (b) 500 hPa pressure level.

developed algorithm. Figure 5 shows CO₂ concentrations retrieved from the clear-sky Band 4 spectra obtained in the daytime from April 6 to 8, 2009. In the daytime, judgment of clear-sky or cloudy conditions is based on the cloud flags provided by the TANSO-CAI. As shown in Figure 5(a), a reasonable latitudinal gradient in CO₂ concentrations can be seen at 770 hPa; CO₂ concentrations over the land in the Northern Hemisphere are higher than those over the ocean and in the Southern Hemisphere. In the middle troposphere, however, evident positive biases exist at low latitudes.

References

- 1) Y. Cui, Y. Mitomi, and T. Takamura, An empirical anisotropy correction model for estimating land surface albedo for radiation budget studies, *Remote Sensing of Environment* 113, 24-39, 2009.
- 2) H. Takenaka, T.Y. Nakajima, I. Okada, J.R. Dim and T. Takamura, Cloud optical thickness estimation from GMS-5/SVSSR, *J. Remote Sensing Soc. Japan*, 29(2), 392-397, 2009.
- 3) Y. Xiong, K. Muramatsu, M. Hirata, K. Oishi, I. Kaihotsu, T. Takamura, S. Furumi and N. Fujiwara, Approximation method for time-integral of photosynthesis for NPP estimation using remote sensing data: case study in Mongolia, *J. Remote Sensing Soc. Japan*, 25(2), 179-190, 2005.
- 4) S. Fukagawa, H. Kuze, G. Bagtasa, S. Naito, M. Yabuki, T. Takamura, N. Takeuchi, Characterization of seasonal and long-term variation of tropospheric aerosols in Chiba, Japan, *Atm. Environ.* 40(12), 2160, 2006.
- 5) T. Takamura, H. Takenaka, Y. Cui, T.Y. Nakajima, A. Higurashi, S. Fukuda, N. Kikuchi, T. Nanakajima, I. Sano and R.T. Pinker, Aerosol and cloud validation system based on SKYNET observations: estimation of shortwave radiation budget using ADEOS II/GLI data, *J. Remote Sensing Soc. Japan*, 29(1), 40-53, 2009.
- 6) G. Bagtasa, C. Liu, N. Takeuchi, H. Kuze, S. Naito, A. Sone, and H. Kan, Dual-site lidar observations and satellite data analysis for regional cloud characterization, *Optical Review*, 14(1), 39-47, 2007.
- 7) J.R. Dim, T. Takamura, I. Okada, T.Y. Nakajima, and H. Takenaka, Influence of inhomogeneous cloud fields on satellite observations, *J. Geophys. Res.*, 112 (D13202), doi:10.1029/2006JD007891, 2007.
- 8) S. Fukagawa, H. Kuze, N. Lagrosas, N. Takeuchi, High-efficiency aerosol scatterometer that uses an integrating sphere for the calibration of multiwavelength lidar data, *Appl. Optics*, 44(17), 3520-3526, 2005.
- 9) N. Lagrosas, H. Kuze, N. Takeuchi, S. Fukagawa, G. Bagtasa, Y. Yoshii, S. Naito, M. Yabuki, Correlation study between suspended particulate matter and portable automated lidar data, *Aerosol Science* 36, 439-454, 2005.
- 10) G. Bagtasa, N. Takeuchi, S. Fukagawa, H. Kuze, S. Naito, Correction in aerosol mass concentration measurements with humidity difference between ambient and instrumental conditions, *Atmospheric Environment* 41, 1616-1626, 2007.
- 11) T. Murayama, S.J. Masonis, J. Redemann, T.L. Anderson, B. Schmid, J.M. Livingston, P.B. Russell, B. Huebert, S.G. Howell, C.S. McNaughton, A. Clarke, M. Abo, A. Shimizu, N. Sugimoto, M. Yabuki, H. Kuze, S. Fukagawa, K.L. Maxwell, R.J. Weber, D.A. Orsini, B. Blomquist, A. Bandy, D. Thornton, An intercomparison of lidar-derived aerosol optical properties with airborne measurements near Tokyo during ACE-Asia, *J. Geophys. Res.*, 108(D23), 6551-8671, 2003.
- 12) D.-H. Kim, B.-J. Sohn, T. Nakajima and T. Takamura, Aerosol radiative forcing over east Asia determined from ground-based solar radiation measurements, *J. Geophys. Res.*, 110, D10S22, doi:10.1029/2004JD004678, 2005.
- 13) T. Takamura, N. Sugimoto, A. Shimizu, A. Uchiyama, A. Yamazaki, K. Aoki, T. Nakajima, B. J. Sohn, and H. Takenaka, Aerosol radiative characteristics at Gosan, Korea, during the Atmospheric Brown Cloud East Asian Regional Experiment 2005, *J. Geophys. Res.*, 112, D22S36, doi:10.1029/2007JD008506, 2007.
- 14) R. Saito, T. Tanaka, H. Hara, H. Oguma, T. Takamura, H. Kuze, and T. Yokota, Aircraft and ground-based observations of boundary layer CO₂ concentration in anticyclonic synoptic condition, *Geophys. Res. Lett.*, 36, L07807, doi:10.1029/2008GL037037, 2009.
- 15) T. Hamazaki, Y. Kaneko, A. Kuze, and K. Kondo, Fourier transform spectrometer for Greenhouse Gases Observing Satellite (GOSAT), *Proc. of Soc. Photo Opt. Instrum. Eng.*, 73-80, 2005.
- 16) A. Kuze, T. Urabe, H. Suto, Y. Kaneko and T. Hamazaki, The instrumentation and the BBM test results of Thermal And Near infrared Sensor for carbon Observation (TANSO) on GOSAT, *Proc. of Soc. Photo Opt. Instrum. Eng.*, 10.1117/12.677113, 2006.
- 17) C.D. Rodgers, Inverse method for atmospheric sounding, World Scientific Publishing, 2000.
- 18) S. Maksyutov, P. K. Patra, R. Onishi, T. Saeki, and T. Nakazawa, NIES/FRCGC global atmospheric tracer transport model: description, validation, and surface sources and sinks inversion, *J. Earth. Sim.*, 9, 3-18, 2008.

19) N. Eguchi, R. Saito, T. Saeki, Y. Nakatsuka, D. Belikov and S. Maksyutov, A priori covariance estimation for CO₂ and CH₄ retrievals, J. Geophys. Res., in revision, 2009.